

## THE ELECTRONIC STRUCTURE OF THE OXYGEN-VACANCY COMPLEX IN SILICON

R. van Kemp, E.G. Sieverts and C.A.J. Ammerlaan  
Natuurkundig Laboratorium der Universiteit van Amsterdam  
Valckenierstraat 65, 1018 XE Amsterdam, The Netherlands

The negatively charged state of the oxygen-vacancy complex in silicon was investigated using electron nuclear double resonance. The unpaired defect electron is mainly located in two dangling bonds in the (0 $\bar{1}$ 1) mirrorplane. In this plane a group of ten tensors was found whose electron densities  $\eta^2$  show a nearly perfect exponential decay as a function of the distance from the centre of the defect in both directions along a [011] zig-zag lattice chain. More than 80% of the defect wave function is localized on these chains. A nearly identical group of tensors exists also for the negative monovacancy in silicon.

### 1. INTRODUCTION

The negatively charged oxygen-vacancy complex (OV $^-$ ) was one of the first radiation damage centres in silicon that was discovered by Electron Paramagnetic Resonance (EPR) [1,2]. This so-called Si-A centre (EPR spectrum B1) is produced by irradiation at room temperature of oxygen-containing n-type silicon with electrons with an energy of 0.5-1.5 MeV.

The identification of the defect was based on the observation that it was produced only in quartz-crucible grown silicon, which is known to contain oxygen to about the maximum solubility, [O] $\approx 10^{18}$  cm $^{-3}$ .

The mechanism for the formation of the defect is that of the capture of a mobile vacancy created during the irradiation by an interstitial oxygen atom. The model for the defect is shown in figure 1.

Electrical measurements of Wertheim [3] showed that the defect acts as an acceptor with a level at  $E_c - 0.17$  eV. From these measurements it was inferred that the complex is in its negative charge state when paramagnetic.

The model for the oxygen-vacancy complex as outlined above was confirmed further by two subsequent papers by Watkins and Corbett [4] and Corbett et al [5]. In the first paper an extensive study of the defect by EPR was presented. An LCAO analysis of the observed hyperfine interactions with the  $^{29}\text{Si}$  nuclei surrounding the defect was given as well as the activation energies for both thermally activated electronic and stress induced atomic reorientation of the complex. In the second paper infrared absorption studies in correlation with

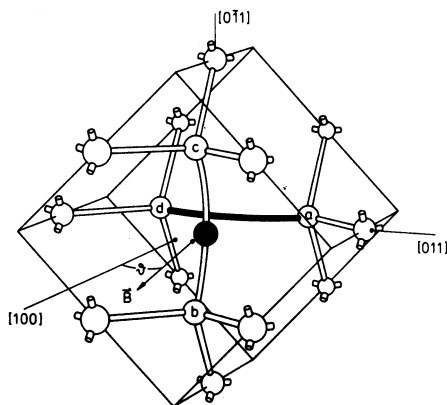


**Figure 1.** Model for the oxygen-vacancy complex. The oxygen atom (black sphere) is located between the atoms b and c; the defect electron is mainly localized between a and d. All further data refer to this standard orientation ad.

Samples were irradiated with 1.5 MeV electrons and beam currents of about  $5 \mu\text{A}\cdot\text{cm}^{-2}$ . The temperature of the sample was kept below  $\sim 70^\circ\text{C}$ .

The EPR and ENDOR measurements were done with a superheterodyne K-band spectrometer operating at 23 GHz. We used a cylindrical  $\text{TE}_{011}$  resonance cavity made of epibond with a silvered inner wall in which a spiral groove was cut, thus acting as an RF coil [6]. ENDOR signals were recorded as changes in the intensity of the dispersion component of the EPR signal using double phase-sensitive detection; the magnetic field was modulated at a frequency of 83.3 Hz and the RF was modulated on-off at a frequency of 3.3 Hz.

The sample was mounted in a stainless steel cryostat that was, among other things, built to function at low temperatures over long periods [7]. The measurements were done at a temperature of 25 K. The magnetic field could be rotated in a  $\{110\}$  plane of the crystal.

### 3. EXPERIMENTAL RESULTS

#### A. EPR

The EPR spectrum of the  $\text{OV}^-$  complex can be described with the spin Hamiltonian

$$\mathcal{H} = \mu_B \vec{B} \cdot \vec{g} \cdot \vec{S}, \quad (1)$$

with  $S=1/2$ . The symmetry of the defect, rhombic I (pointgroup  $2mm$ ), is reflected in the form of the  $g$ -tensor, which for this symmetry has three independent parameters. The principal values of the  $g$ -tensor were calculated by a computer fit of the measured magnetic resonance fields to equation (1). The values thus found were:  $g_1 = 2.0033 \pm 0.0001$  ( $\parallel [100]$ ),  $g_2 = 2.0025 \pm 0.0001$  ( $\parallel [011]$ ), and  $g_3 = 2.0093 \pm 0.0001$  ( $\parallel [0\bar{1}1]$ ), in good agreement with reference [4]. Figure 2 shows the angular plot of the effective  $g$ -values,  $g_{\text{eff}}$ , for rotation of the magnetic field in the  $(0\bar{1}1)$ -plane. The six different defect orientations are labelled in accordance with figure 1.

EPR measurements were presented.

In this paper we will present the results of a study by electron nuclear double resonance (ENDOR) of hyperfine interactions with  $^{29}\text{Si}$  nuclei. In particular we will focus on a group of hyperfine interaction tensors that gives remarkable microscopic information about the electronic structure of the defect. It appeared that this group of tensors is nearly identical to a group found for the negative monovacancy.

In section 2 we will give a description of the experimental procedure; in section 3 experimental results will be presented and they will be discussed in section 4.

### 2. EXPERIMENTAL PROCEDURE

Experiments were performed on n-type silicon (typical dimensions  $2 \times 2 \times 20 \text{ mm}^3$ ) with a phosphorus concentration  $[\text{P}] \approx 9 \times 10^{17} \text{ cm}^{-3}$ . The oxygen concentration was about  $5 \times 10^{17} \text{ cm}^{-3}$ .

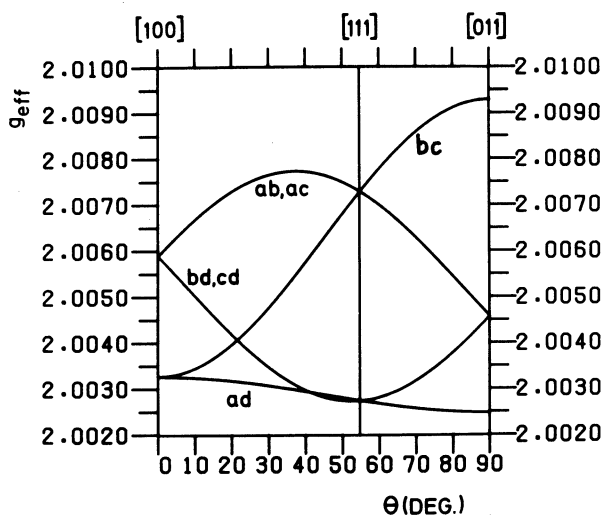


Figure 2. Angular dependence of the effective g-values,  $g_{\text{eff}}$ , of the  $OV^-$  complex for rotation of the magnetic field  $\vec{B}$  in the  $(0\bar{1}1)$ -plane. Orientation labels refer to figure 1.

### B. ENDOR

The ENDOR spectra can be described with the spin Hamiltonian

$$H = \mu_B \vec{B} \cdot \vec{g} \cdot \vec{S} + \sum_i (\vec{S} \cdot \vec{A}_i \cdot \vec{I}_i - g_N \mu_N \vec{B} \cdot \vec{I}_i), \quad (2)$$

with  $S=1/2$  and  $I=1/2$ .

To the electron Zeeman interaction term in equation (1), are added the interaction of the defect electron with  $^{29}\text{Si}$  nuclei and the nuclear Zeeman interaction, respectively. The index  $i$  enumerates the lattice sites around the defect.

The configuration  $(OV^- + ^{29}\text{Si})$  can have three different symmetries, that are reflected in the hyperfine interaction tensor  $A$ : triclinic, monoclinic I and rhombic I (pointgroups 1,  $m$  and  $2mm$ , respectively). Symmetry equivalent atoms form so-called shells. For the monoclinic shells we can discriminate between shells in the  $ad=(0\bar{1}1)$  and  $bc=(011)$  mirrorplanes. Angular dependent ENDOR scans were made for the defect orientations labelled  $ad$  and  $bc$  in figure 2. Together with the ENDOR frequencies obtained for the other orientations in the  $[100]$  and  $[011]$  directions, a sufficient set of frequencies is obtained to determine a specific hyperfine tensor uniquely. The hyperfine tensor parameters were determined by a computer fit to equation (2). In these fits the  $g$ -values were kept constant and the nuclear Zeeman interaction term was taken to be isotropic with  $g_N \mu_N / h = -8.458778 \text{ MHz} \cdot \text{T}^{-1}$  [7]. Line widths at half maximum (FWHM) varied from about 2 kHz in the low-frequency region to about 350 kHz for the largest hyperfine interaction. From the  $Mad$  class shells a group of ten can be distinguished which show a remarkable similarity to each other. This group will be discussed in the next section. Figure 3 shows the largest hyperfine interaction tensor of this group, which is also resolved in EPR, as well as the smallest hyperfine tensor.

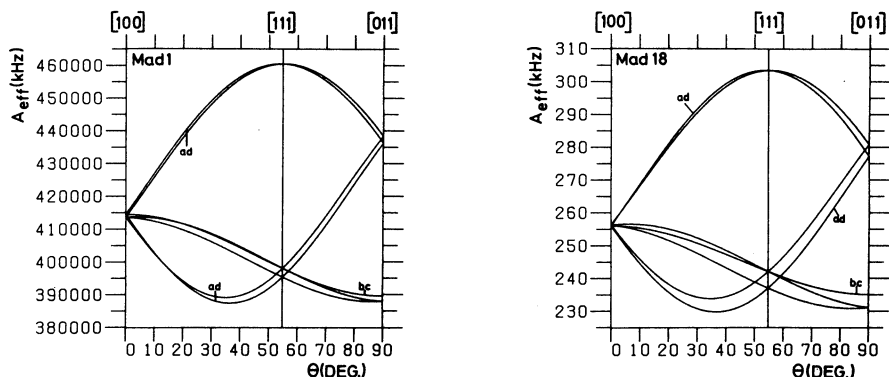


Figure 3. Angular dependences of the effective A-values for the largest hyperfine interaction Mad1 (left) and the smallest one, Mad18, of the group of tensors. Note that they both have nearly axial symmetry.

#### 4. DISCUSSION

In the model for the defect, that was proposed by Watkins and Corbett [4], the defect electron is thought to occupy an antibonding orbital. The wave function of the electron is constructed from the orbitals centered on the four nearest neighbours of the vacancy. With this model it is found that the wave function is mainly located on the atoms a and d. This is confirmed by experiment; about 60% of the wave function is found to be localized on these two atoms. The remaining 40% is spread out over the more distant silicon neighbours.

For an LCAO wave function  $\Psi = \sum_i \eta_i (\alpha_i \psi_s^i + \beta_i \psi_p^i)$  it follows that hyperfine interaction tensors are axially symmetric and can be written as the sum of an isotropic part, the Fermi contact interaction, and an anisotropic part, the dipole-dipole interaction

$$\vec{A}_i = a_i \vec{1} + \vec{B}_i. \quad (3)$$

The Fermi contact interaction is written as

$$a_i = \frac{2}{3} \mu_0 g \mu_B g_N \mu_N \eta_i^2 \alpha_i^2 |\Psi(0)|_s^2, \quad (4)$$

with  $a_i = \frac{1}{3} \text{Tr}(\vec{A}_i)$ . The dipole-dipole interaction tensor has principal values  $(2b_i, -b_i, -b_i)$ , with:

$$b_i = \frac{\mu_0}{4\pi} g \mu_B g_N \mu_N \eta_i^2 \beta_i^2 \langle r^{-3} \rangle_p. \quad (5)$$

The parameter  $\eta_i^2$  is the fraction of the wave function centered at site  $i$ ;  $\alpha_i^2$  and  $\beta_i^2$  are respectively the fraction s- and p-character. Normalization requires that  $\alpha_i^2 + \beta_i^2 = 1$ . Atomic orbital parameters  $|\Psi(0)|_s^2 = 34.5 \times 10^{30} \text{ m}^{-3}$  and  $\langle r^{-3} \rangle_p = 18.6 \times 10^{30} \text{ m}^{-3}$  can be taken from reference [8]. Using these values and the experimental parameters  $a_i$  and  $b_i$ , we calculated the parameters  $\alpha_i^2$ ,  $\beta_i^2$  and  $\eta_i^2$ . These values and those for  $a_i$  and  $b_i$  are given in table I for the group of ten Mad tensors (the complete results will be published in a subsequent paper [9]). For this defect with rhombic I symmetry, axially symmetric tensors actually do not exist. For these ten tensors the deviation is small, however, so that the LCAO description gives a very good approximation.

**Table I.** LCAO parameters for the group of selected Mad tensors. As the sign of the hyperfine interactions could not be determined, absolute values for  $a$  are given. Parameters are defined as in the text.  $\Delta A$  is the absolute error. Lattice positions are given as [xyy]. Equivalent positions are [ $x\bar{y}\bar{y}$ ]. Tensors that do not belong to the subgroup of Mad tensors are omitted.

Tensor	$a$ (kHz)	$b$ (kHz)	$a/b$	$\Delta A$ (kHz)	$\alpha^2$ (%)	$\beta^2$ (%)	$\eta^2$ (%)	Position
Mad1	412476	23980	17.2	10	30.2	69.8	30.0	[111]
Mad2	39393	4087	9.6	5	19.5	80.5	4.4	[022]
Mad3	26116.5	2840.1	9.2	1	18.8	81.2	3.1	[133]
Mad4	17582.5	1428.7	12.3	0.6	23.6	76.4	1.6	[044]
Mad5	6399	655	9.8	3.0	19.7	80.3	0.71	[155]
Mad6	3395.7	344.4	9.9	0.2	19.9	80.1	0.38	[066]
Mad8	1617.8	145.1	11.2	0.3	21.9	78.1	0.16	[177]
Mad9	1056.1	94.7	11.2	0.3	21.9	78.1	0.16	[088]
Mad13	384.0	39.5	9.7	0.1	19.6	80.4	0.04	[199]
Mad18	256.1	23.7	10.8	0.4	21.3	78.7	0.03	[01010]

The tensors listed in table I are selected as they are very similar to each other in the following aspects:

- the largest principal value has its axis nearly parallel to  $\langle 111 \rangle$ , the second-largest principal value has its axis perpendicular to the Mad mirrorplane,
- the ratio  $a/b$  is very similar for all the tensors,
- the deviation from axiality is only about 10% for all of them.

The ten other Mad class tensors that we found are appreciably different in these aspects. Within the group only Mad1 is somewhat exceptional. A possible explanation for this can be found in inward distortions of the nearest-neighbours of the vacancy.

It can be seen that subsequent values of  $\eta^2$  differ roughly by a factor of two (with Mad1 again as an exception). Figure 4 shows a semi-logarithmic plot of  $\eta^2$ -values from table I versus the distance to the vacancy of successive lattice sites on the zig-zag chain along a  $\langle 110 \rangle$  direction measured along the bonds.

All the points can be fitted to a straight line of the form

$$\eta^2(r_i) = \eta_0^2 \exp(-r_i/r_0) . \quad (6)$$

Leaving out Mad1 this gave  $\eta_0^2 = 0.20$  and  $r_0 = 3.5 \text{ \AA}$  with a correlation coefficient 0.993.

We conclude that the assumption seems justified that the tensors of table I should be identified with lattice sites on the two semi-infinite chains of atoms along the [011] and [0 $\bar{1}\bar{1}$ ] directions starting at the vacancy. This is not unreasonable since the electron density is mainly located on the two nearest-neighbour atoms and in a covalent lattice the wave function has a preference to propagate along the bonds. The complete assignment is shown in table I.

The model for the electronic structure of the  $OV^-$  complex that emerges from above considerations is that of an extended quasi one-dimensional defect; ~80% of the electron density is confined to the chains of atoms that lie along the [011] and [0 $\bar{1}\bar{1}$ ] directions emanating from the centre of the defect. Along these chains the electron density falls off exponentially at a rather slow rate. Under the present assignment tensor Mad18 measures the interaction with atoms at a distance as far as 19.2  $\text{\AA}$ .

Experimental support for this model is found in the ENDOR measurements on the negatively charged monovacancy (EPR spectrum Si-G2) by Sprenger et al [7,10,11]. This defect has the same symmetry and comparable  $g$ -values. Also here a similar group of ten Mad tensors with the same characteristics as

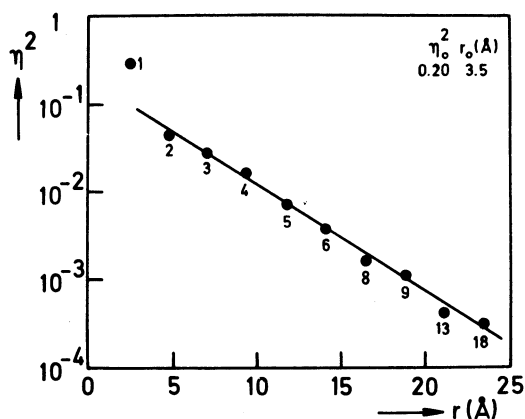


Figure 4. Localization  $\eta^2$  as a function of distance  $r$  along the [011]-chain of atoms. Numbers refer to the Mad tensors of table I.

perturbation potential, a preference for the electronic charge to spread out along the twelve  $\langle 110 \rangle$  lattice chains was found. From Kane's data a decay length of the charge on the chain atoms of  $r_0 = 3.4 \text{ \AA}$  can be derived. This value is in very good agreement with the present experimental data.

#### ACKNOWLEDGEMENTS

RvK would like to thank Dr. M. Sprenger for suggesting the experiment and for the many enthusiastic discussions. This work was supported by the Dutch Foundation for Fundamental Research on Matter (FOM).

#### REFERENCES

- [1] Bemski, G., *J. Appl. Phys.* **30**, 1195 (1959).
- [2] Watkins, G.D., Corbett, J.W., and Walker, R.M., *J. Appl. Phys.* **30**, 1198 (1959).
- [3] Wertheim, G.K., *Phys. Rev.* **105**, 1730 (1957); *Phys. Rev.* **110**, 1272 (1958).
- [4] Watkins, G.D. and Corbett, J.W., *Phys. Rev.* **121**, 1001 (1961).
- [5] Corbett, J.W., Watkins, G.D., Chrenko, R.M., and McDonald, R.S., *Phys. Rev.* **121**, 1015 (1961).
- [6] Ludwig, G.W. and Woodbury, H.H., *Phys. Rev.* **117**, 102 (1960).
- [7] Sprenger, M., Ph.D. thesis, 1986, University of Amsterdam.
- [8] Morton, J.R. and Preston, K.F., *J. Magn. Resonance* **30**, 577 (1978).
- [9] van Kemp, R. et al, to be published.
- [10] Sprenger, M., Muller, S.H., and Ammerlaan, C.A.J., *Physica* **116B**, 224 (1983).
- [11] Sprenger, M., Muller, S.H., Sieverts, E.G., and Ammerlaan, C.A.J., accepted for publication in *Phys. Rev. B*.
- [12] Sieverts, E.G., *J. Phys. C: Solid State Phys.* **14**, 2217 (1981).
- [13] Kane, E.O., *Phys. Rev.* **B31**, 5199 (1985).

mentioned for the group of Mad tensors of table I was found. Sprenger analyzed his results in the same fashion as was proposed earlier by Sieverts for the analysis of the ENDOR measurements on the positively and negatively charged states of the divacancy in silicon [12], the difference being that Sprenger took the particular group of similar tensors as in the present case. A fit of Sprenger's data on the vacancy gave a very comparable result:  $\eta_0^2 = 0.27$  and  $r_0 = 3.3 \text{ \AA}$ . This is one of the indications that vacancy and oxygen-vacancy complex are defects with a similar electronic structure.

Theoretical support for the "chain-model" for both  $V^-$  and  $OV^-$  is found in calculations by Kane [13]. For a defect with cubic symmetry and taking a simple